FLARE FEATURES OF AR LACERTAE

R. K. SRIVASTAVA

Uttar Pradesh State Observatory, Manora Peak, Naini Tal, India

(Received 2 September, 1985)

Abstract. BV optical flares of AR Lacertae, found in 1979 observations, are presented and their features are discussed. The effect of wave migration and the significance levels of flares originating around both eclipses have been estimated. Flare features suggest that both the components of AR Lac have spotted regions and show activity. The varying amplitudes of flares indicate varying degrees of activity. These results are well supported by observations in other wavelength regions.

1. Introduction

The system AR Lac (= BD + 45°3813) was discovered to be a variable by Leavitt (1903). Its eclipsing binary nature has been confirmed by many authors (cf. Srivastava, 1981). Harper (1933) noted that the secondary (K0) component of the system AR Lac had sharp H and K emission lines, while Kron (1947) found 'star spots' on the photosphere of the primary (G5) component of the system. Struve (1952) explained the spectra of the system based on the 'turbulent spot' hypothesis.

The RS CVn-type eclipsing binary AR Lac is an active system. The presence of Ca II H and K emissions, Hα emissions, X-rays, radio flares, spot activity, circular polarization, and magnetic field has been detected by several investigators as described earlier (cf. Srivastava, 1981, 1983, 1984a, b, 1985; Goraya and Srivastava, 1984). Kiziloğlu *et al.* (1983), from UV observations, detected both chromospheric and transition region lines and commented on their variability. Walter *et al.* (1983), from X-ray observations, described the coronal structure of the components of AR Lac. Doiron and Mutel (1984) from dual-frequency radio observations detected the existence of the magnetic field in the system, and found significant circular polarization (2–8%).

Much has been said about the activity of the system AR Lac from UV, X-ray, and radio observations, but almost nothing is known in the optical region except the observations of Ca II H and K emissions and Hα emissions. This is third paper in a series regarding the detection of optical (*U*, *B*, and *V*) flares associated with the system. Our two earlier papers presented some optical flares of the system and their characteristics (cf. Srivastava, 1983, 1985). Goraya and Srivastava (1984), from spectral scans, reported the variation of Ca II H and K and Hα emission lines in an interval as short as three minutes. More recently, we have found that even less than two minutes variability of Ca II H and K and Hα emissions is detectable.

2. Method for the Detection of Light Variations

The variable light was noticeable in the *B* and *V* observations secured in the year 1979 (cf. Kurutaç *et al.*, 1981). The changes in the light level of AR Lac have been separated

Astrophysics and Space Science **120** (1986) 239–252.

TABLE I

Flare observations of AR Lacertae

Phase	*B* filter			Phase	*V* filter		
	MIL (Δm)	QIL (Δm)	Flare (Δm) O–C		MIL (Δm)	QIL (Δm)	Flare (Δm) O–C
			J.D. 2444065				
0.372	1.040	1.040	0.000	0.364	0.625	0.625	0.000
0.373	1.047	1.040	+0.007	0.365	0.633	0.625	+0.008
0.374	1.053	1.040	+0.013	0.366	0.643	0.625	+0.018
0.375	1.060	1.040	+0.020	0.367	0.653	0.625	+0.028
0.376	1.061	1.039	+0.022	0.368	0.657	0.624	+0.033
0.377	1.063	1.039	+0.024	0.369	0.662	0.624	+0.038
0.378	1.066	1.040	+0.026	0.370	0.666	0.625	+0.041
0.379	1.067	1.039	+0.028	0.371	0.667	0.625	+0.042
0.380	1.066	1.040	+0.026	0.372	0.665	0.625	+0.040
0.381	1.065	1.040	+0.025	0.373	0.663	0.625	+0.038
0.382	1.059	1.040	+0.019	0.374	0.658	0.625	+0.033
0.383	1.056	1.040	+0.016	0.375	0.652	0.625	+0.027
0.384	1.052	1.040	+0.012	0.376	0.644	0.625	+0.019
0.385	1.048	1.040	+0.008	0.377	0.633	0.625	+0.008
0.386	1.043	1.040	+0.003	0.378	0.625	0.625	0.000
0.387	1.041	1.040	+0.001	–	–	–	–
0.388	1.040	1.040	0.000	–	–	–	–
			J.D. 2444108				
0.966	0.450	445	+0.005	0.966	0.103	0.092	+0.011
0.967	0.425	423	+0.003	0.967	0.075	0.070	+0.005
0.968	0.415	415	0.000	0.968	0.048	0.057	−0.009
0.969	0.373	380	−0.007	0.969	0.035	0.038	−0.003
0.970	0.323	365	−0.032	0.970	0.027	0.032	−0.005
0.971	0.313	335	−0.022	0.971	0.010	0.012	−0.002
0.972	0.308	315	−0.007	0.972	0.005	−0.002	−0.007
0.973	0.295	290	+0.005	0.973	−0.008	−0.022	+0.014
0.974	0.290	270	+0.020	0.974	−0.010	−0.035	+0.025
0.975	0.282	0.257	+0.025	0.975	−0.025	−0.038	+0.013
0.976	0.275	0.242	+0.033	0.976	−0.035	−0.042	+0.007
0.977	0.270	0.238	+0.032	0.977	−0.023	−0.040	+0.017
0.978	0.255	0.228	+0.027	0.978	−0.025	−0.050	+0.025
0.979	0.248	0.230	+0.018	0.979	−0.023	−0.055	+0.032
0.980	0.246	0.231	+0.015	0.980	−0.022	−0.057	+0.035
0.981	0.250	0.232	+0.018	0.981	−0.030	−0.055	+0.025
0.982	0.255	0.228	+0.027	0.982	−0.037	−0.053	+0.016
0.983	0.258	0.223	+0.035	0.983	−0.027	−0.051	+0.024
0.984	0.267	0.215	+0.042	0.984	−0.020	−0.047	+0.027
0.985	0.263	0.213	+0.050	0.985	−0.025	−0.053	+0.028
0.986	0.267	0.214	+0.053	0.986	−0.025	−0.052	+0.027
0.987	0.267	0.215	+0.052	0.987	−0.027	−0.053	+0.026
0.988	0.262	0.212	+0.050	0.988	−0.025	−0.049	+0.024
0.989	0.253	0.211	+0.042	0.989	−0.021	−0.048	+0.027
0.990	0.252	0.213	+0.039	0.990	−0.020	−0.050	+0.030
0.991	0.258	0.215	+0.043	0.991	−0.018	−0.051	+0.033

Table I (continued)

Phase	*B* filter			Phase	*V* filter		
	MIL (Δm)	QIL (Δm)	Flare (Δm) O–C		MIL (Δm)	QIL (Δm)	Flare (Δm) O–C
0.992	0.262	0.218	+ 0.044	0.992	− 0.015	− 0.051	+ 0.036
0.993	0.267	0.220	+ 0.047	0.993	− 0.013	− 0.051	+ 0.038
0.994	0.272	0.222	+ 0.050	0.994	− 0.012	− 0.052	+ 0.040
0.995	0.275	0.221	+ 0.054	0.995	− 0.008	− 0.052	+ 0.044
			J.D. 2444113				
–	–	–	–	0.468	0.430	0.430	0.000
–	–	–	–	0.469	0.423	0.425	− 0.002
0.470	0.837	0.837	0.000	0.470	0.413	0.420	− 0.007
0.471	0.830	0.832	− 0.002	0.471	0.400	0.413	− 0.013
0.472	0.825	0.820	− 0.005	0.472	0.392	0.407	− 0.015
0.473	0.820	0.820	0.000	0.473	0.384	0.404	− 0.020
0.474	0.810	0.813	− 0.003	0.474	0.385	0.397	− 0.012
0.475	0.799	0.807	− 0.008	0.475	0.385	0.390	− 0.005
0.476	0.790	0.802	− 0.012	0.476	0.387	0.387	0.000
0.477	0.786	0.795	− 0.009	0.477	0.390	0.383	+ 0.007
0.478	0.785	0.789	− 0.004	0.478	0.390	0.377	+ 0.013
0.479	0.784	0.782	− 0.002	0.479	0.393	0.376	+ 0.017
0.480	0.782	0.781	+ 0.001	0.480	0.387	0.367	+ 0.020
0.481	0.782	0.779	+ 0.003	0.481	0.377	0.363	+ 0.014
0.482	0.779	0.774	+ 0.005	0.482	0.367	0.360	+ 0.007
0.483	0.782	0.771	+ 0.011	0.483	0.362	0.358	+ 0.004
0.484	0.775	0.768	+ 0.007	0.484	0.363	0.356	+ 0.007
0.485	0.770	0.766	+ 0.004	0.485	0.358	0.348	+ 0.010
0.486	0.768	0.759	+ 0.009	0.486	0.357	0.345	+ 0.012
0.487	0.768	0.757	+ 0.011	0.487	0.357	0.343	+ 0.014
0.488	0.765	0.753	+ 0.012	0.488	0.355	0.342	+ 0.013
0.489	0.765	0.751	+ 0.014	0.489	0.351	0.341	+ 0.010
0.490	0.764	0.749	+ 0.015	0.490	0.351	0.343	+ 0.008
0.491	0.761	0.747	+ 0.014	0.491	0.339	0.337	+ 0.002
0.492	0.761	0.748	+ 0.013	0.492	0.337	0.337	0.000
0.493	0.753	0.744	+ 0.009	0.493	0.330	0.333	− 0.003
0.494	0.747	0.743	+ 0.004	0.494	0.336	0.335	+ 0.001
0.495	0.744	0.742	+ 0.002	0.495	0.337	0.334	+ 0.003
0.496	0.746	0.740	+ 0.006	0.496	0.336	0.331	+ 0.005
0.497	0.749	0.739	+ 0.010	0.497	0.338	0.330	+ 0.008
0.498	0.751	0.738	+ 0.013	0.498	0.347	0.330	+ 0.017
0.499	0.749	0.738	+ 0.011	0.499	0.344	0.329	+ 0.015
0.500	0.747	0.737	+ 0.010	0.500	0.342	0.329	+ 0.013
0.501	0.748	0.739	+ 0.009	0.501	0.340	0.329	+ 0.011
0.502	0.748	0.740	+ 0.008	0.502	0.340	0.332	+ 0.008
0.503	0.743	0.737	+ 0.006	0.503	0.335	0.330	+ 0.005
0.504	0.739	0.736	+ 0.003	0.504	0.338	0.330	+ 0.008
0.505	0.744	0.736	+ 0.008	0.505	0.345	0.330	+ 0.015
0.506	0.748	0.737	+ 0.011	0.506	0.348	0.330	+ 0.018
0.507	0.749	0.737	+ 0.012	0.507	0.350	0.331	+ 0.019
0.508	0.748	0.738	+ 0.010	0.508	0.351	0.331	+ 0.020
0.509	0.747	0.739	+ 0.008	0.509	0.341	0.332	+ 0.009

Table I (continued)

Phase	*B* filter			Phase	*V* filter		
	MIL (Δm)	QIL (Δm)	Flare (Δm) O–C		MIL (Δm)	QIL (Δm)	Flare (Δm) O–C
0.510	0.746	0.740	+ 0.006	0.510	0.337	0.334	+ 0.003
0.511	0.745	0.741	+ 0.004	0.511	0.336	0.336	0.000
0.512	0.745	0.743	+ 0.002	0.512	0.332	0.334	− 0.002
0.513	0.748	0.745	+ 0.003	0.513	0.340	0.336	− 0.004
0.514	0.750	0.746	+ 0.004	0.514	0.341	0.337	+ 0.004
0.515	0.752	0.747	+ 0.005	0.515	0.346	0.338	+ 0.008
0.516	0.750	0.746	+ 0.004	0.516	0.351	0.340	+ 0.011
0.517	0.757	0.754	+ 0.003	0.517	0.350	0.342	+ 0.008
0.518	0.762	0.757	+ 0.005	0.518	0.350	0.344	+ 0.006
0.519	0.766	0.757	+ 0.009	0.519	0.350	0.347	+ 0.003
0.520	0.767	0.759	+ 0.008	0.520	0.350	0.350	0.000
0.521	0.769	0.762	+ 0.007	0.521	0.356	0.354	+ 0.002
0.522	0.773	0.767	+ 0.006	0.522	0.360	0.355	+ 0.005
0.523	0.775	0.770	+ 0.005	0.523	0.365	0.357	+ 0.008
0.524	0.778	0.773	+ 0.004	0.524	0.372	0.362	+ 0.010
0.525	0.788	0.781	+ 0.007	0.525	0.376	0.367	+ 0.009
0.526	0.792	0.782	+ 0.010	0.526	0.379	0.373	+ 0.006
0.527	0.797	0.789	+ 0.008	0.527	0.382	0.378	+ 0.004
0.528	0.800	0.795	+ 0.005	0.528	0.388	0.385	+ 0.003
0.529	0.804	0.802	+ 0.002	0.529	0.395	0.387	+ 0.008
0.530	0.810	0.810	0.000	0.530	0.409	0.397	+ 0.012
0.531	0.812	0.813	− 0.001	0.531	0.422	0.405	+ 0.017
0.532	0.825	0.819	+ 0.006	0.532	0.422	0.407	+ 0.015
0.533	0.840	0.826	+ 0.014	0.533	0.427	0.415	+ 0.012
0.534	0.857	0.838	+ 0.019	0.534	0.438	0.422	+ 0.016
0.535	0.863	0.840	+ 0.023	0.535	0.448	0.428	+ 0.020
0.536	0.867	0.846	+ 0.021	0.536	0.460	0.435	+ 0.025
0.537	0.872	0.852	+ 0.020	0.537	0.460	0.443	+ 0.017
0.538	0.877	0.858	+ 0.019	0.538	0.460	0.450	+ 0.010
0.539	0.885	0.868	+ 0.017	0.539	0.465	0.463	+ 0.002
0.540	0.885	0.872	+ 0.013	0.540	0.470	0.476	− 0.006
0.541	0.887	0.877	+ 0.010	0.541	0.475	0.475	0.000
0.542	0.890	0.882	+ 0.008	0.542	0.489	0.490	+ 0.001
0.543	0.895	0.890	+ 0.005	0.543	0.495	0.498	− 0.003
0.544	0.899	0.897	+ 0.002	0.544	0.495	0.502	− 0.007
0.545	0.902	0.903	− 0.001	0.545	0.498	0.507	− 0.009
0.546	0.909	0.908	− 0.002	0.546	0.502	0.513	− 0.011
0.547	0.914	0.910	− 0.004	0.547	0.515	0.523	− 0.008
			J.D. 2444114				
0.953	0.670	0.678	− 0.008	0.953	0.293	0.310	− 0.017
0.954	0.662	0.657	+ 0.005	0.954	0.288	0.295	− 0.007
0.955	0.650	0.637	+ 0.013	0.955	0.285	0.285	0.000
0.956	0.640	0.617	+ 0.023	0.956	0.275	0.270	+ 0.005
0.957	0.623	0.605	+ 0.018	0.957	0.250	0.240	+ 0.010
0.958	0.605	0.590	+ 0.015	0.958	0.245	0.230	+ 0.015
0.959	0.560	0.555	+ 0.005	0.959	0.234	0.227	+ 0.007
0.960	0.548	0.550	− 0.002	0.960	0.205	0.200	+ 0.005

Table I (continued)

Phase	*B* filter			Phase	*V* filter		
	MIL (Δm)	QIL (Δm)	Flare (Δm) O–C		MIL (Δm)	QIL (Δm)	Flare (Δm) O–C
0.961	0.550	0.545	+ 0.005	0.961	0.185	0.185	0.000
0.962	0.505	0.510	− 0.005	0.962	0.172	0.165	+ 0.007
0.963	0.487	0.485	+ 0.003	0.963	0.170	0.158	+ 0.012
0.964	0.483	0.475	+ 0.008	0.964	0.153	0.137	+ 0.016
0.965	0.483	0.471	+ 0.012	0.965	0.132	0.105	+ 0.027
0.966	0.468	0.445	+ 0.023	0.966	0.122	0.092	+ 0.030
0.967	0.455	0.425	+ 0.030	0.967	0.097	0.070	+ 0.027
0.968	0.425	0.415	+ 0.010	0.968	0.070	0.057	+ 0.013
0.969	0.385	0.380	+ 0.005	0.969	0.045	0.038	+ 0.007
0.970	0.365	0.365	0.000	0.970	0.033	0.032	+ 0.001
0.971	0.345	0.335	+ 0.010	0.971	0.023	0.012	+ 0.011
0.972	0.340	0.315	+ 0.025	0.972	0.020	0.000	+ 0.020
0.973	0.320	0.290	+ 0.030	0.973	0.005	− 0.022	+ 0.027
0.974	0.303	0.270	+ 0.033	0.974	− 0.002	− 0.035	+ 0.033
0.975	0.290	0.255	+ 0.035	0.975	− 0.015	− 0.038	+ 0.023
0.976	0.276	0.240	+ 0.036	0.976	− 0.013	− 0.040	+ 0.027
0.977	0.272	0.240	+ 0.032	0.977	− 0.017	− 0.047	+ 0.030
0.978	0.272	0.220	+ 0.052	0.978	− 0.015	− 0.050	+ 0.035
0.979	0.284	0.227	+ 0.057	0.979	− 0.022	− 0.055	+ 0.033
0.980	0.285	0.230	+ 0.050	0.980	− 0.028	− 0.057	+ 0.029
0.981	0.275	0.232	+ 0.043	0.981	− 0.035	− 0.055	+ 0.020
0.982	0.275	0.228	+ 0.047	0.982	− 0.040	− 0.053	+ 0.013
0.983	0.275	0.223	+ 0.052	0.983	− 0.030	− 0.052	+ 0.022
0.984	0.276	0.215	+ 0.061	0.984	− 0.023	− 0.050	+ 0.027
0.985	0.278	0.213	+ 0.065	0.985	− 0.018	− 0.053	+ 0.035
0.986	0.276	0.212	+ 0.064	0.986	− 0.013	− 0.050	+ 0.037
0.987	0.273	0.210	+ 0.063	0.987	− 0.018	− 0.053	+ 0.035
0.988	0.272	0.210	+ 0.062	0.988	− 0.020	− 0.054	+ 0.034
0.989	0.268	0.211	+ 0.057	0.989	− 0.017	− 0.050	+ 0.033
0.990	0.267	0.213	+ 0.054	0.990	− 0.008	− 0.048	+ 0.040
0.991	0.275	0.215	+ 0.060	0.991	− 0.004	− 0.047	+ 0.043
0.992	0.285	0.218	+ 0.067	0.992	− 0.006	− 0.051	+ 0.045
0.993	0.280	0.220	+ 0.060	0.993	− 0.010	− 0.051	+ 0.041
0.994	0.273	0.222	+ 0.051	0.994	− 0.013	− 0.052	+ 0.039
0.995	0.270	0.221	+ 0.049	0.995	− 0.008	− 0.052	+ 0.044
0.996	0.271	0.216	+ 0.055	0.996	− 0.002	− 0.048	+ 0.046
0.997	0.270	0.212	+ 0.058	0.997	− 0.009	− 0.057	+ 0.048
0.998	0.272	0.210	+ 0.062	0.998	− 0.011	− 0.060	+ 0.049
0.999	0.275	0.209	+ 0.066	0.999	− 0.005	− 0.055	+ 0.050
0.000	0.280	0.210	+ 0.070	0.000	− 0.002	− 0.053	+ 0.051
0.001	0.280	0.212	+ 0.068	0.001	− 0.005	− 0.052	+ 0.047
0.002	0.283	0.214	+ 0.069	0.002	− 0.007	− 0.052	+ 0.045
0.003	0.285	0.217	+ 0.068	0.003	− 0.009	− 0.053	+ 0.044
0.004	0.286	0.219	+ 0.067	0.004	− 0.012	− 0.055	+ 0.043
0.005	0.286	0.221	+ 0.065	0.005	− 0.013	− 0.053	+ 0.040
0.006	0.287	0.223	+ 0.064	0.006	− 0.013	− 0.050	+ 0.037
0.007	0.290	0.224	- 0.066	0.007	− 0.012	− 0.043	+ 0.031
0.008	0.290	0.222	+ 0.068	0.008	− 0.015	− 0.043	+ 0.028

Table I (continued)

Phase	*B* filter			Phase	*V* filter		
	MIL (Δm)	QIL (Δm)	Flare (Δm) O–C		MIL (Δm)	QIL (Δm)	Flare (Δm) O–C
0.009	0.290	0.220	+0.070	0.009	−0.010	−0.042	+0.032
0.010	0.290	0.217	+0.073	0.010	−0.010	−0.045	+0.035
0.011	0.290	0.215	+0.075	0.011	−0.010	−0.047	+0.037
0.012	0.286	0.212	+0.076	0.012	−0.011	−0.043	+0.032
0.013	0.288	0.213	+0.075	0.013	−0.013	−0.038	+0.025
0.014	0.289	0.215	+0.074	0.014	−0.015	−0.032	+0.017
0.015	0.290	0.217	+0.073	0.015	−0.017	−0.032	+0.015
0.016	0.289	0.220	+0.069	0.016	−0.013	−0.033	+0.020
0.017	0.290	0.228	+0.062	0.017	−0.010	−0.040	+0.030
0.018	0.290	0.231	+0.059	0.018	−0.007	−0.045	+0.038
0.019	0.290	0.236	+0.054	0.019	+0.002	−0.043	+0.045
0.020	0.295	0.235	+0.060	0.020	0.020	−0.038	+0.058
0.021	0.299	0.235	+0.064	0.021	0.030	−0.033	+0.063
0.022	0.309	0.238	+0.071	0.022	0.030	−0.035	+0.065
0.023	0.318	0.240	+0.078	0.023	0.033	−0.035	+0.068
0.024	0.313	0.248	+0.065	0.024	0.040	−0.030	+0.070
0.025	0.324	0.271	+0.053	0.025	0.050	−0.025	+0.075
0.026	0.332	0.287	+0.045	0.026	0.060	−0.018	+0.078
0.027	0.355	0.313	+0.042	0.027	0.075	−0.001	+0.076
0.028	0.382	0.342	+0.040	0.028	0.087	0.018	+0.069
0.029	0.398	0.363	+0.035	0.029	0.095	0.033	+0.062
0.030	0.415	0.382	+0.033	0.030	0.115	0.055	+0.060
0.031	0.430	0.400	+0.030	0.031	0.118	0.063	+0.055
0.032	0.452	0.425	+0.027	0.032	0.128	0.080	+0.048
0.033	0.472	0.450	+0.022	0.033	0.160	0.115	+0.045
0.034	0.485	0.475	+0.010	0.034	0.173	0.132	+0.040
0.035	0.505	0.500	+0.005	0.035	0.188	0.153	+0.035
0.036	0.520	0.520	0.000	0.036	0.205	0.175	+0.030
0.037	0.530	0.540	−0.010	0.037	0.225	0.198	+0.027
0.038	0.545	0.565	−0.020	0.038	0.235	0.210	+0.025
0.039	0.575	0.585	−0.010	0.039	0.250	0.233	+0.017
0.040	0.600	0.600	0.000	0.040	0.262	0.248	+0.014
0.041	0.620	0.625	−0.005	0.041	0.273	0.263	+0.010
0.042	0.640	0.640	0.000	0.042	0.280	0.285	+0.005
0.043	0.655	0.654	+0.001	0.043	0.290	0.292	−0.002
0.044	0.670	0.670	0.000	0.044	0.307	0.307	0.000

out using the technique described earlier (cf. Srivastava, 1983, 1985). The *B* and *V* observations of 1979 suggested some variation in the light of the AR Lac system during totality. On plotting all the observations, it was found that the observations of four nights (J.D. 2444065, J.D. 2444108, J.D. 2444113, and J.D. 2444114) showed deviations from the light curves drawn through all the observations. These deviations, MIL–QIL (Maximum Intensity Level–Quiescent Intensity Level) denoted as O–C, of *B* and *V* light curves have been obtained at a phase interval of 0.001, and are given in Table I

and plotted in Figure 1(a)–(b) and 2(a)–(b). The solid points represent the flare-like activity raising the intensity above the quiescent intensity level; the open circles are the points obtained by simple O–C calculation, which help in gaining an idea about the start and end times of various flares. The solid curves in the figures represent QIL, and the dips indicate the spotted regions. The reading error of MIL and QIL magnitudes is not greater than $0^m.001$. The wave migration effect is investigated in the light of the fact that the system AR Lac is an Algol-type eclipsing binary. The wave migration effect is estimated in Section 4.

3. Source of Light Variations

The presence of gas streaming, pulsation or intrinsic variability, the existence of the extended atmosphere around the components, the wave migration effect, and the presence of spots or flare activity can change the depths and or light levels. The humps and asymmetries in the branches of minima are not apparent in the light curves, hence, gas streaming can not account for these features. The duration of the totality does not apparently change from night to night, nor is any change of the totality is apparent in the present and 1982 observations, as described in the text, hence, the possibility of pulsation or intrinsic variability is also ruled out. The dips are not seen before the first and after the fourth contact of the eclipses; hence, the presence of an extended atmosphere around the components of the system is also impossible. Thus, either the wave migration effect or spot or flare activity may cause the light variations present in the system.

4. Effect of the Wave Migration and Significance Level

Figures 1(a)–(b) reveal that the positions of spots have not changed between the observations of J.D. 2444108 and J.D. 2444114 (i.e., in a six-day interval), which suggests that the wave is not migrating fast. Since dips are seen at the tips of both the primary and of the secondary minima, we infer that both components of AR Lac have spotted regions and are active. Our this finding is supported by the observations of Kiziloğlu *et al.* (1983). This finding of ours is also supported by the observations of Everen *et al.* (1983), who have found two maxima of the migration wave, but not two minima, which should have been the case. Kurutaç *et al.* (1981) have shown that the minimum of the wave is centred at 0.0 phase, i.e., at the time of the primary minimum. Since the light of only the secondary (larger) component is found here, we are, therefore, seeing the maximum spotted hemisphere of the secondary component at this phase. Kiziloğlu *et al.* (1983) have shown that the faces of the two stars away from each other are more active. Thus, the maximum spotted hemisphere of the primary component must lie at phase 0.5, i.e., at the time of the secondary minimum. Now, if we assume that both components are equally active, as nearly the same number of spots is seen during the totality and during the annularity region, and assume that the migrating waves emanating from both components are symmetrical, then their effects will cancel one

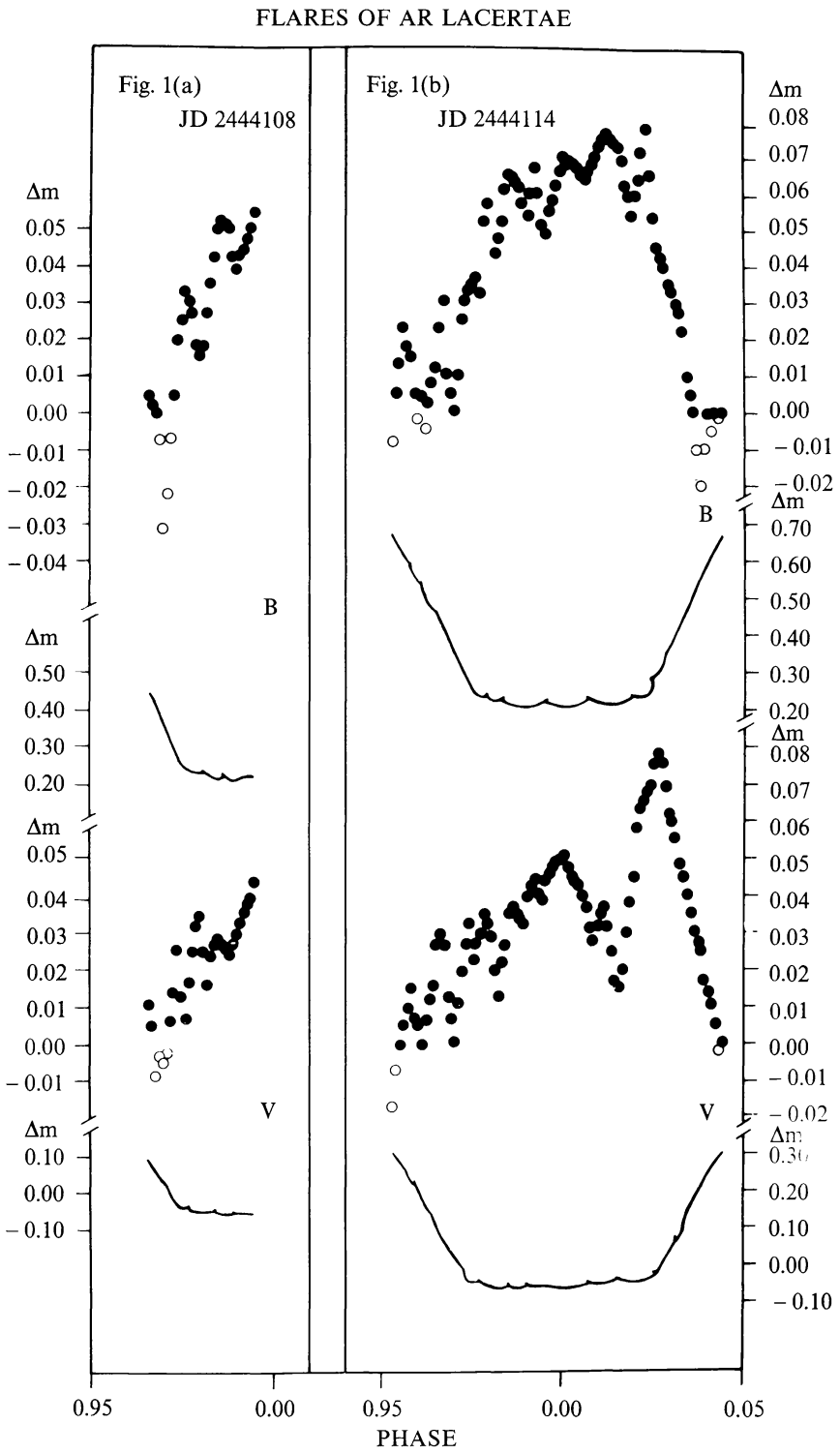

Fig. 1(a)–(b). Flares of AR Lacertae around the phase of primary minimum.

TABLE II

Characteristics of flares of AR Lacertae

Min.	J.D.	Filter	Start time of flare	End time of flare	Duration of flare in phase	Duration of flare in hours	Phase of flare maximum	Maximum amplitude of flare (m)
Sec.	2444065	*B*	0.372	0.388	0.016	00^h23^m	0.379	0.028[c]
		V	0.364	0.378	0.014	00 20	0.371	0.042[c]
					First flare			
Pr.	2444108	*B*	0.970	0.980	0.010	00 29	0.976	0.033[b]
		V	0.968	0.976	0.008	00 23	0.974	0.025[b]
					Second flare			
		B	0.980	0.990	0.010	00 29	0.986	0.052[b]
		V	0.976	0.982	0.006	00 17	0.986	0.052[b]
					Third flare			
		B	0.990	0.995	0.005	00 14	–	0.054[b]
		V	0.982	0.995	0.013	00 37	–	0.043[b]
					First flare			
Sec.	2444113	*V*	0.473	0.483	0.010	00 29	0.480	0.020[b]
					Fourth flare			
		V	0.503	0.513	0.010	00 29	0.508	0.020[b]
					Eight flare			
		B	0.531	0.547	0.016	00 46	0.535	0.023[c]
		V	0.534	0.546	0.012	00 32	0.536	0.025[c]
					First flare			
Pr.	2444114	*B*	0.953	0.962	0.009	00 26	0.956	0.023[b]
					Second flare			
		B	0.962	0.970	0.008	00 23	0.966	0.030[b]
		V	0.961	0.970	0.009	00 26	0.967	0.030[b]
					Third flare			
		B	0.970	0.977	0.007	00 20	0.974	0.036[b]
		V	0.970	0.975	0.005	00 14	0.976	0.033[b]
					Fourth flare			
		B	0.977	0.981	0.004	00 11	0.979	0.057[b]
		V	0.975	0.982	0.007	00 20	0.978	0.035[b]
					Fifth flare			
		B	0.981	0.990	0.009	00 26	0.985	0.065[b]
		V	0.982	0.989	0.007	00 20	0.986	0.038[b]

Table II (continued)

Min. J.D.	Filter	Start time of flare	End time of flare	Duration of flare in phase	Duration of flare in hours	Phase of flare maximum	Maximum amplitude of flare (m)
			Sixth flare				
	B	0.990	0.995	0.005	00 14	0.992	0.067[b]
	V	0.989	0.994	0.005	00 14	0.992	0.045[b]
			Seventh flare				
	B	0.995	0.006	0.011	00 32	0.000	0.070[b]
	V	0.994	0.008	0.014	00 40	0.000	0.051[b]
			Eighth flare				
	B	0.006	0.019	0.013	00 37	0.012	0.076[b]
	V	0.008	0.015	0.007	00 20	0.011	0.037[b]
			Ninth flare				
	B	0.019	0.044	0.025	01 12	0.023	0.078[b]
	V	0.015	0.044	0.029	01 23	0.026	0.078[a]

[a] Nearly complete flare.
[b] Incomplete flare.
[c] Complete flare.

another out. Since Kiziloğlu *et al.* (1983) have shown that the primary and the secondary components contribute 32 and 68% of the total activity, respectively, the differential effect of both waves must be 36%. Kiziloğlu *et al.* (1983) stated that during the distortion wave minimum 34% higher line fluxes are found than the fluxes of the distortion wave maximum. Considering this to be a differential wave flux enhancement, and considering the differential effect given above, we may assume that differential wave effect is 35% on the average. Around the times of the primary and the secondary minima, the amplitudes of flares ranges from $0^m.025$ to $0^m.078$ and $0^m.020$ to $0^m.042$ (see Table II), respectively. Assuming the differential wave effect of 35%, these amplitude ranges are affected by $0^m.009$ to $0^m.027$ and $0^m.007$ to $0^m.015$. (It is evident that the maximum effect on the migration wave around the primary and the secondary eclipses is $\sim 0^m.03$ and $\sim 0^m.02$. In addition, the photometric observational error is nowhere more than $0^m.01$. Kurutaç *et al.* (1981) have shown that the amplitude of the wave increased by about $0^m.03$ in one year, which suggests that the amplitude of the wave is changing. The present estimates of the wave effect around the phase of primary minimum lies near to the amplitude change.) These are, therefore, the significance levels of the flares. In any case, at the phases of the primary and the secondary minima, flares possessing amplitudes greater than $0^m.027$ and $0^m.015$, respectively, are significant.

5. Description and the Discussion of Flares

The flare-like features of four nights are shown in Figures 1(a)–(b) and 2(a)–(b), and their characteristics are given in Table II. These characteristics are reported as the mean of B and V filters for the purposes of detailed discussion.

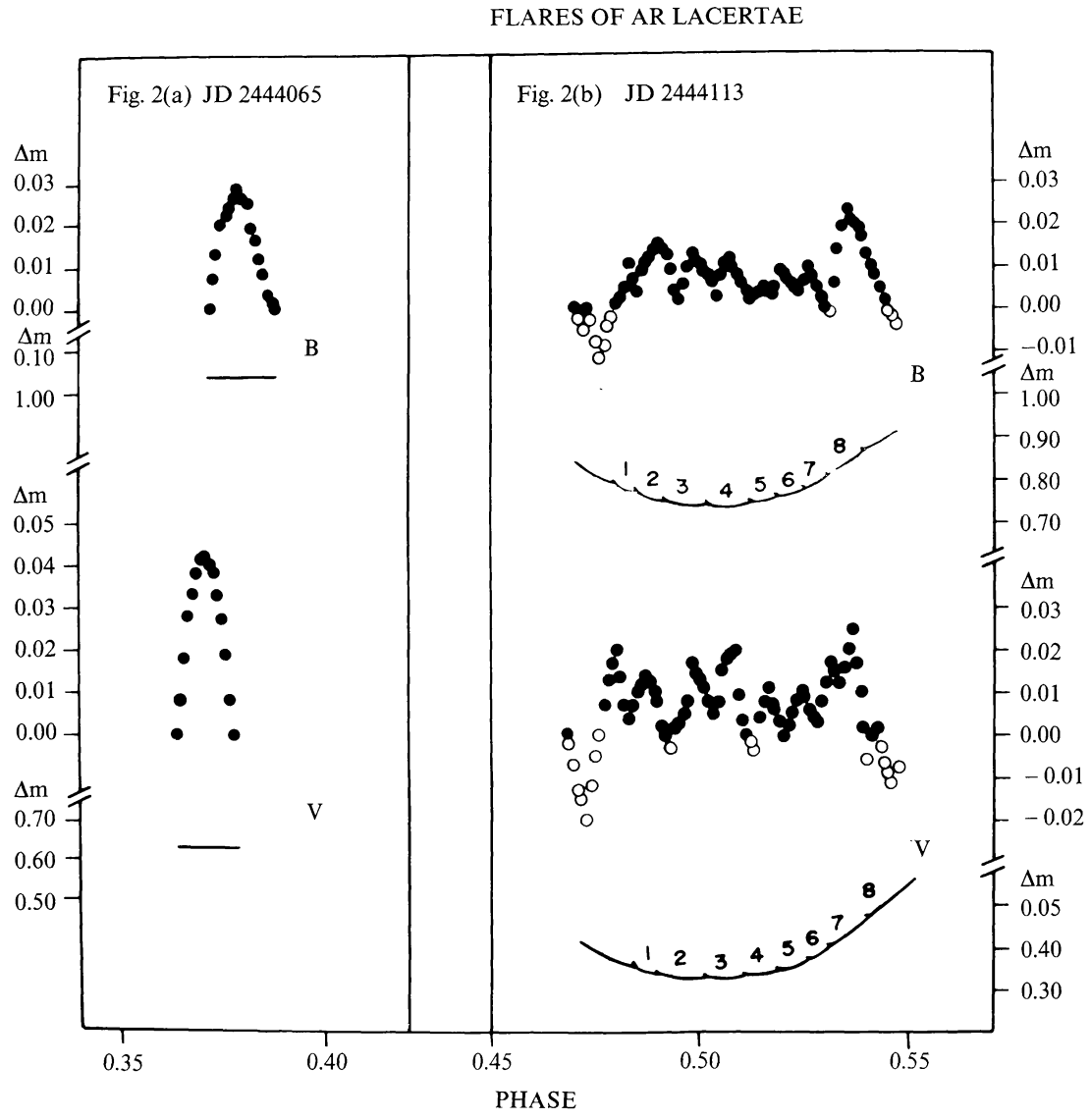

Fig. 2(a)–(b). Flares of AR Lacertae outside and around the phase of secondary minimum.

The flare pattern of J.D. 2444065 depicts a single complete flare which ascends above the quiescent intensity level (QIL) at phase 0.368, rises sharply, reaches maximum (flare) intensity level (MIL) at phase 0.375, possessing an amplitude of $0^m.035$, then subsides comparatively less sharply to the quiescent intensity level at phase 0.383. It lies outside the first contact of the secondary minimum, hence, it may be emanating from either of

the components. Comparison with the flare patterns given by Kiziloğlu *et al.* (1983), taken two days later than these observations on J.D. 2444067 suggests that the more active secondary component is responsible for this flare. This conclusion is further supported by the ΔK_1 index, the ratio of the baseline widths of K_1 and K_2 emission features given by Naftilan and Aikman (1981), indicating that between phases 0.365 and 0.385 the secondary component is more active than the primary.

The flare pattern of J.D. 2444108 suggests that it consists of three flares. The first flare appears to begin at phase 0.969, but actually ascends sharply from the QIL at phase 0.973, reaches maximum intensity level (MIL) at phase 0.975, with an amplitude of $0^m.029$, then declines sharply till phase 0.978, but does not return to QIL. From this phase, the second flare begins to rise sharply, reaches MIL at phase 0.983, with an amplitude of $0^m.044$, then sharply declines until phase 0.986 without touching QIL. From here, the third flare starts more slowly than earlier flares, and ascends until phase 0.995. The flare is incomplete, and at its lasting phase it has an amplitude of $0^m.049$. The primary minimum plot of J.D. 2444114 suggests that the region of totality lies between phases 0.9745 and 0.0255 (or ± 0.0255), which is nearly the same – within graphical error – as found in 1982. Thus the duration of totality has not changed. In the QIL curve three dips are seen, corresponding to the above-mentioned flares. The shapes of the first and the second flares, when compared to the flare patterns of J.D. 2444114, especially in the *B* filter, suggest that these may be connected with the primary component, as they show sharp rise and sharp decline; while the third flare, which definitely lies in the totality region, may originate from the more active secondary component. But Figure 1(a) shows that all these flares and their corresponding dips lie in the totality region, hence, it is inferred that all three flares originate from the secondary component only, whose light is available at the time of totality.

The flare pattern of J.D. 2444113 indicates that there are, in all, eight flares, whose amplitudes above the QIL range from $0^m.010$ to $0^m.025$; corresponding to these flares there are eight dips in the QIL curve. Looking at their shapes, it is apparent that four of them show a sharp rise and slow decline, and the remaining four show a slow rise and slow decline. On comparison with the shapes of flare features given by Kiziloğlu *et al.* (1983), it is inferred that former flares may originate from the secondary component, and the latter four from the primary. The amplitudes of these flares are not appreciable, hence, except for a few, we consider them as flare-like fluctuations.

The flare pattern of J.D. 2444114 presents the most interesting features, which suggest that there are, in all, nine flares, and corresponding to these, there are nine dips in the QIL curve. The first flare appears to start sharply from phase 0.953 but actually ascends above the QIL at phase 0.955, reaches MIL at phase 0.957 with an amplitude of $0^m.019$, then slowly declines till phase 0.962 without subsiding to QIL. The second flare starts from here, rises sharply, reaches MIL at phase 0.967 with an amplitude of $0^m.030$, then declines sharply till phase 0.970 without touching QIL. The third flare begins sharply from here, reaches MIL at phase 0.975 with an amplitude of $0^m.038$, then declines sharply till phase 0.976, not reaching the QIL. From this phase, the fourth flare rises slowly, reaches MIL at phase 0.979 with an amplitude of $0^m.046$, then declines

sharply till phase 0.985 without returning to QIL. From here, the fifth flare begins to ascend sharply, reaches MIL at phase 0.986 with an amplitude of $0^m.052$, then declines slowly till phase 0.990 without descending to QIL. The sixth flare ascends sharply from here, reaches MIL at phase 0.992 with an amplitude of $0^m.056$, then declines sharply till phase 0.995, not returning to QIL. The seventh flare starts sharply from here, reaches MIL at phase 0.000 (at mid-primary eclipse) with an amplitude of $0^m.061$, then declines slowly till phase 0.007 without touching QIL. From phase 0.007, the eighth flare rises sharply, reaches MIL at phase 0.012 with an amplitude of $0^m.057$, then declines sharply till phase 0.017 without returning to QIL. From here, the ninth strongest flare ascends slowly, having the largest duration, reaches MIL at phase 0.025 with an amplitude of $0^m.078$, touches QIL at phase 0.039, and appears to descend further till phase 0.044. The first, second, and ningth flares lie outside the totality region, so may be contributed by either of the components, while the remaining six flares lie in the totality region and are emanate from the secondary component only, whose light is available here. It is possible that the first and the second flares may be originate from the primary and the secondary components, respectively, as we can see on comparing their pattern to those of Kiziloğlu *et al.* (1983); the first flare shows a sharp rise and slow decline, while the second indicates a slow rise and slow decline. It is possible that the contributions of flares from both components may have merged in the ninth flare. Since, corresponding to six flares lying in the totality region there are six dips, indicative of six spot centers, it is possible that these spot centers may contribute to six magnetic loops, and may be forming a long-lived flare, as suggested by Walter *et al.* (1980) in connection with the coronal loops; alternatively these flares can be treated as the consecutive flares emanating from the cooler component.

6. Conclusions

Except the ninth flare of J.D. 2444114, which has an amplitude of $0^m.078$ and a duration of 78 min, the ranges of the amplitudes and the durations of flares are $0^m.010$ to $0^m.057$, and 11 min to 40 min, respectively. Since the shapes and sizes of the flares are changing even for the same phase, and the amplitudes are randomly varying, and short-term changes are noticed in the features of flares emerging from both the minima, we infer that both components of AR Lac are active and possess active and dynamic chromospheres. These conclusions are supported by the Ca II H and K observations of Naftilan and Aikman (1981), who showed that the emission strength for both components was randomly but continually variable. Our results are also supported by the Mg II h and k observations of Kiziloğlu *et al.* (1983). Goraya and Srivastava (1984) reported short-term changes (as short as 3 min) in the emission features of Ca II H and K emission and Hα emission features, and changes as short as 11 min are now found. The short-term random variation of these flare features suggests that the variations are due to outbursts of activity in the chromosphere of the components. The occasionally enhanced chromospheric activity, as seen in the ninth flare of J.D. 2444114, may be linked with large-scale flaring (cf. Naftilan and Aikman, 1981).

7. Remarks

It is important to note that the system was active in 1973 (cf. Hjellming and Blankenship, 1973; Gibson and Hjellming, 1974). It was active in the 1975–1976 observing season (cf. Naftilan and Drake, 1977; Rhombs and Fix, 1977; Srivastava, 1983), and showed activity in 1982 (cf. Doiron and Mutel, 1984; Srivastava, 1985). Its activity in 1979 has been presented here. It will be worth while to monitor continuously AR Lac at all possible wavelengths in the 1985–1986 observing season to see if the system shows considerable activity and to ascertain if any correlation exists between the activity and the phase. The technique of finding optical flares, which we have elaborated, will be useful in future. The observations of flares around several primary and secondary minima will help in understanding the nature of the activity of the individual components.

To sum up, we have detected optical flares of AR Lac in 1975–1976, 1979, and 1982; others found flares of the system in 1973. If such activity is found in 1985, it will help in understanding whether or not a spot cycle of a decade or so is operating in the system.

References

Doiron, D. J. and Mutel, R. L.: 1984, *Astron. J.* **89**, 430.
Everen, S., Ibanoğlu, C., Tümer, O., Tunca, Z., and Ertan, A. Y.: 1983, *Astrophys. Space Sci.* **95**, 401.
Gibson, D. M. and Hjellming, R. M.: 1974, *Publ. Astron. Soc. Pacific* **86**, 652.
Goraya, P. S. and Srivastava, R. K.: 1984, *Inf. Bull. Var. Stars*, No. 2579.
Harper, W. E.: 1933, *J. Roy. Astron. Soc. Canada* **27**, 146.
Hjellming, R. M. and Blankenship, L.: 1973, *Nature Phys. Sci.* **243**, No. 127, 81.
Kiziloğlu, Ü., Derman, E., Ögelman, H., and Tokdemir, F.: 1983, *Astron. Astrophys.* **123**, 17.
Kron, G. E.: 1947, *Publ. Astron. Soc. Pacific* **59**, 261.
Kurutaç, M., Ibanoğlu, C., Tunca, Z., Ertan, A. Y., Everen, S., and Tümer, O.: 1981, *Astrophys. Space Sci.* **77**, 325.
Leavitt, H.: 1903, *Harvard Circ.*, No. 130, 4.
Naftilan, S. A. and Aikman, G. C. L.: 1981, *Astron. J.* **86**, 766.
Naftilan, S. A. and Drake, S. A.: 1977, *Astrophys. J.* **216**, 508.
Rhombs, C. G. and Fix, J. D.: 1977, *Astrophys. J.* **216**, 503.
Srivastava, R. K.: 1981, *Astrophys. Space Sci.* **78**, 123.
Srivastava, R. K.: 1983, *Inf. Bull. Var. Stars*, No. 2450.
Srivastava, R. K.: 1984a, *Bull. Astron. Soc. India* **12**, 52.
Srivastava, R. K.: 1984b, *Acta Astron.* **34**, No. 2, 291.
Srivastava, R. K.: 1985, in press.
Struve, O.: 1952, *Publ. Astron. Soc. Pacific* **64**, 20.
Walter, F. M., Cash, W., Charles, P., and Bowyer, P.: 1980, *Astrophys. J.* **236**, 212.
Walter, F. M., Gibson, D. M., and Basri, G. S.: 1983, *Astrophys. J.* **267**, 665.